Journal of Sound and Vibration (2002) **256**(2), 249–270
doi:10.1006/jsvi.2001.4205, available online at http://www.idealibrary.com on IDEAL®

IDENTIFICATION OF MODAL PARAMETERS FROM MEASURED OUTPUT DATA USING VECTOR BACKWARD AUTOREGRESSIVE MODEL

C. F. Hung and W. J. Ko

Department of Naval Architecture and Ocean Engineering, National Taiwan University, 73 Chow-Shan Road, Taipei, Taiwan, Republic of China. E-mail: hungef@ccms.ntu.edu.tw

(*Received* 6 *August* 2001, *and in final form* 16 *November* 2001)

In this paper, a modal identification system that is based on the vector backward autoregressive (VBAR) model has been developed for the identification of natural frequencies, damping ratios and mode shapes of structures from measured output data. The modal identification using forward autoregressive approach has some problems in discriminating the structure modes from spurious modes. On the contrary, the VBAR approach provides a determinate boundary for the separation of system modes from spurious modes, and an eigenvalue filter for the selection of physical modes is existent in the proposed method. For convenience of application, the backward state equation established from VBAR model is transformed into a forward state equation, which is termed as transformed VFAR model in this paper. In addition, the extraction of equivalent system matrix of state equation of motion for structures from the transformed VFAR model has been developed, and then the normal modes can be calculated from the identified equivalent system matrix. Two examples of modal identification are carried out to demonstrate the availability and effectiveness of the proposed backward approach: (1) Numerical modal identification for a three-degree-of-freedom dynamic system with noise level in 20% of r.m.s of measured output data; (2) experimental modal identification of a cantilever beam. Finally, to show the advantage of the proposed VBAR approach on the selection of physical modes, the modal identification by stochastic subspace method was performed. The results from both methods are compared.

1. INTRODUCTION

In practical design for vibration control or model updating of structural system, the modal parameters provide important information on dynamic properties. During the past few decades, various methods for identification of modal parameters have been developed. According to the processing domain, the modal identification can be categorized into time-domain and frequency-domain methods. The frequency domain methods have become popular, and are still predominant in engineering practice [1, 2]. The time-domain methods are useful for problems with large number of modes from multi-channel measurement, also useful for closely spaced and non-proportional modes. The time-domain or frequency-domain methods have their merits in extracting modal parameters from measured data. The time-domain methods can directly address the measured response data; hence this paper focuses on the time-domain methods.

The works on time-domain method began in the late 1970s, such as the Ibrahim time-domain method [3, 4] and the polyreference method [5–7]. The eigensystem

0022-460X/02/$35.00

realization algorithm (ERA) proposed by Juang and Pappa [8, 9] can identify the state-space model from impulse response. The Prony signal analysis method [10] and the time series model [11–13] have been proposed in the last decade to identify modal parameters in various engineering fields.

In order to improve the accuracy of identified modal parameters for measured data with noise, the overspecified model order is a popular approach among the time-domain methods. Discriminating physical modes from spurious modes and then reducing the overspecified models to an equivalent physical model play a key role for further applications. The singular value decomposition based methods such as eigensystem realization algorithm and stochastic subspace algorithm [14, 15] employ the dominant singular value of preselected block Hankel matrix to identify the order of the model. When the signal-to-noise ratio (SNR) is not high enough and the noise level may outperform some physical modes, the singular value decomposition based methods suffer from difficulties in the selection of the number of dominant singular value. Cremona and Brandon [16] mentioned that the order determination by singular value decomposition method is a totally subjective technique for estimating the number of modes, and can lead to incorrect results in the presence of high level of noise. Therefore, some reprocessing techniques or prior knowledge of structures may be required to discriminate structure modes from spurious modes. Peterson and Alvin [17] proposed a combination of several quantitative modal quality indicators (MQI) to discriminate unwanted modes.

This paper concentrates on the time series model to extract the modal parameters from measured output data. There are two kinds of time series models, one is the auto-regressive moving average (ARMA) model, and the other is the auto-regressive (AR) model. The maximum likelihood (ML) method for the estimation of the parameters of ARMA model is very complicated, and requires optimization of the highly non-linear likelihood functions [18]. Li and Ko [11] employed iterative and computationally expensive sub-optimal techniques to determine the parameters of ARMA model. In addition, the likelihood function may be characterized by a number of local extreme values that may lead to errant results, initial guesses for the estimation of parameters are also required, and computational instabilities may occur.

There are various schemes to overcome these shortcomings. The simplest way is the adoption of a higher order of AR model in place of an ARMA model [13, 19–21]. The high order AR model has high number of eigenvalues; only some of them are physical modes. The selection of physical modes and the reduction of the high order model to a physical model become key problems. He and Roeck [20] fitted the observed data to a series of models with different orders and plotted the final prediction error diagrams. The method determines the range of model order only and further refinement of the model is necessary. Kumaresan and Tufts [22] proposed a backward prediction model to identify the frequencies and damping factors from single-channel response data. Hollkamp and Batill [23] developed a single-input–single-output backward time series model to predict the transient response of the sailplane subject to arbitrary inputs. Cooper [24] used a backward prediction error model to identify the natural frequencies and damping factors from single channel response data. It showed that the backward model has an advantage in the separation of physical modes from spurious modes. Because all eigenvalues computed from a forward AR model using least-squares technique always locate inside the unit circle, the separation of system eigenvalues from spurious eigenvalues needs some additional technique, like Wahab and Roeck [25]. On the contrary, the system eigenvalues computed by backward model will locate outside or on the unit circle, and the non-system eigenvalues lie inside the unit circle.

Both VFAR and VBAR models can process only output data, which are free response data or forced response data under white noise type of exciting force. Huang [26] used VFAR model to identify the dynamic characteristics of a structure from ambient vibration measurement. In this paper, a vector backward auto-regressive (VBAR) model is proposed for the mode selection and parameter estimation. For convenience of application, the backward state equation established from VBAR model can be transformed into a forward state equation. The system matrices of the transformed VFAR model are different from common VFAR model.

2. MULTIVARIATE BACKGROUND AR MODEL

The p-variate time series data, $y_t \in R^{p\times 1}$, which are measured from p-channels on a structure at time t, can be approximated by the following multivariate backward AR model:

$$y_t = \sum_{i=1}^{q} a_i y_{t+i} + \varepsilon_t = a_1 y_{t+1} + a_2 y_{t+2} + \cdots + a_q y_{t+q} + \varepsilon_t; \quad t = 1 \text{ to } N, \tag{1}$$

where the subscript t is the discrete time index, N is the number of observed time steps, q is the order of AR model, and ε_t is the backward prediction error. In this model, the current time series data are expressed as a linear combination of the time series data in the next future steps and the backward prediction error. The prediction error is assumed to be a white noise with zero mean. This difference model in equation (1) is called the p-variate, q-order vector backward autoregressive model, which is represented by VBAR (p, q). The parameter matrices shown in equation (1), $a_i \in R^{p\times p}$, are termed as the backward AR parameter matrices, which contain the dynamic characteristics of structural system. The time series data in equation (1) can be assembled from time step $t = 1$ to $N - q$, and the following linear matrix equation can be established:

$$[y_1 \;\; y_2 \;\; \cdots \;\; y_{N-q}] = [a_1 \;\; a_2 \;\; \cdots \;\; a_q] \begin{bmatrix} y_2 & y_3 & \cdots & y_{N-q+1} \\ y_3 & y_4 & \cdots & y_{N-q+2} \\ \vdots & \vdots & & \vdots \\ y_{q+1} & y_{q+2} & \cdots & y_N \end{bmatrix} + [\varepsilon_1 \;\; \varepsilon_2 \;\; \cdots \;\; \varepsilon_{N-q}]. \tag{2}$$

The AR parameter matrices can be solved by least-squares method. The eigenvalues of the backward model can be evaluated by its characteristic matrix polynomial as follows [27]:

$$P_b(\lambda) = I_p \lambda^q - a_1 \lambda^{q-1} - \cdots a_{q-1}\lambda - a_q = 0_p \tag{3}$$

where I_p and 0_p are $p \times p$ the identity and null matrices respectively. If the signal-to-noise ratio is not high enough in the observed time series data, then the estimation of eigenvalues from AR models will be disturbed by measurement noise. Therefore, how to improve the accuracy of the estimated eigenvalues for noisy measurements is a problem of great concern. An effective method is to overspecify the order of model.

A state vector, $z_t = [y_t^{\mathrm{T}} \;\; y_{t+1}^{\mathrm{T}} \;\; \cdots \;\; y_{t+q-1}^{\mathrm{T}}]^{\mathrm{T}} \in R^{pq \times 1}$, consisting of the output vector of q-time steps is introduced and the following state-space equation can be obtained:

$$z_t = \begin{bmatrix} a_1 & \cdots & a_{q-1} & a_q \\ I_p & \cdots & 0_p & 0_p \\ \vdots & & \vdots & \vdots \\ 0_p & 0_p & I_p & 0_p \end{bmatrix} z_{t+1} + \begin{bmatrix} I_p \\ 0_p \\ \vdots \\ 0_p \end{bmatrix} \varepsilon_t \tag{4a}$$

or in compact matrix form

$$z_t = A'_d z_{t+1} + B'_d \varepsilon_t \tag{4b}$$

The backward difference model described in equation (1) can also be rewritten as follows:

$$y_t = [a_1 \;\; a_2 \;\; \cdots \;\; a_q] z_{t+1} + \varepsilon_t \tag{5a}$$

or

$$y_t = C'_d z_{t+1} + D'_d \varepsilon_t \tag{5b}$$

Equations (4b) and (5b) are the state equation and output equation of VBAR model respectively. The characteristic polynomial of the system matrix A'_d is the same as equation (3).

In experimental modal identification, the analysis frequency bandwidth of the structure is dependent on the sampling rate of measured data. Although the number of vibration modes for a continuous structure is theoretically infinite, only the modes within the analysis bandwidth can be identified correctly. If the measured data for a structure contains n vibration modes, it will have n-pairs of conjugate system eigenvalues in state equation of motion. A VAR model with p-channels and q-order for a structure has pq eigenvalues. Usually, pq is much higher than $2n$, and the order of VBAR model must be selected such that $q \geqslant 2n/p$, otherwise the wrong results may be obtained or some modes will be lost. The $2n$ system eigenvalues can be picked out from the pq eigenvalues. To establish the physical state equation of motion and to determine the modal parameters, the $pq - 2n$ spurious modes should be removed from the pq-modes of state equation.

For convenience of application, the backward state-space model can be transformed into the forward model. When both sides of equation (4b) are multiplied by $A_d'^{-1}$, the state vector z_{t+1} can be written as

$$z_{t+1} = A_d'^{-1} z_t - A_d'^{-1} B'_d \varepsilon_t = \bar{A}_d z_t + \bar{B}_d \varepsilon_t. \tag{6}$$

Substituting the above equation into equation (5b), the output equation can be rewritten into its forward form as follows:

$$\begin{aligned} y_t &= C'_d z_{t+1} + D'_d \varepsilon_t \\ &= C'_d (A_d'^{-1} z_t - A_d'^{-1} B'_d \varepsilon_t) + D'_d \varepsilon_t \\ &= C'_d A_d'^{-1} z_t + (D'_d - C'_d A_d'^{-1} B'_d) \varepsilon_t \\ &= \bar{C}_d z_t + \bar{D}_d \varepsilon_t. \end{aligned} \tag{7}$$

Equations (6) and (7) are the state equation and output equation of transformed vector forward AR model that is called TVFAR model in this paper. The VBAR and TVFAR systems can be represented by the coefficient matrices sets (A'_d, B'_d, C'_d, D'_d) and $(\bar{A}_d, \bar{B}_d, \bar{C}_d, \bar{D}_d)$ respectively. From equations (4) and (6), the system matrix of transformed forward state-space model is expressed as follows:

$$\bar{A}_d = A_d'^{-1} = \begin{bmatrix} 0_p & I_p & \cdots & 0_p \\ \vdots & \vdots & \vdots & \vdots \\ 0_p & 0_p & \cdots & I_p \\ a_q^{-1} & -a_q^{-1}a_1 & \cdots & -a_q^{-1}a_{q-1} \end{bmatrix}. \tag{8}$$

The relationships between the transformed forward and backward state-space matrices are

$$\bar{A}_d = A_d'^{-1}, \tag{9a}$$

$$\bar{B}_d = -A_d'^{-1}B'_d = [0_p \ \cdots \ 0_p \ -a_q^{-1}], \tag{9b}$$

$$\bar{C}_d = C'_d A_d'^{-1} = [I_p \ 0_{p\times(q-1)}], \tag{9c}$$

$$\bar{D}_d = D'_d - C'_d A_d'^{-1} B'_d = 0_p. \tag{9d}$$

The characteristic polynomial of the transformed forward state system matrix is

$$p_f(\bar{\lambda}) = I_p\bar{\lambda}^q + a_q^{-1}a_{q-1}\bar{\lambda}^{q-1} + \cdots + a_q^{-1}a_1\bar{\lambda} - a_q^{-1} = 0_p. \tag{10}$$

When both sides of equation (10) are multiplied by $-a_q\bar{\lambda}^{-q}$, the eigenvalue $\bar{\lambda}$ is not changed, equation (10) can be rewritten as

$$-a_q - a_{q-1}\bar{\lambda}^{-1} - \cdots - a_1\bar{\lambda}^{1-q} + I_p\bar{\lambda}^{-q} = 0_p. \tag{11}$$

Comparing equation (3) with (11), it is clear that $\lambda = \bar{\lambda}^{-1}$, i.e., the eigenvalues associated with the characteristic polynomial of TVFAR model are the reciprocal of the eigenvalues associated with VBAR model.

From equation (3), the eigenvalues of the backward state-space system matrix can be decomposed as

$$p_b(\lambda) = \prod_{k=1}^{pq}(\lambda - \lambda_k) = \prod_{i=1}^{2n}(\lambda - \lambda_i)\prod_{j=1}^{pq-2n}(\lambda - \lambda_j) = 0. \tag{12a}$$

Kumaresan and Tufts [22] pointed out that the magnitudes of the eigenvalues of backward model are

$$|\lambda_i| \geqslant 1{\cdot}0 \ \text{ for } i \leqslant 2n, \quad \text{and} \quad |\lambda_i| < 1{\cdot}0 \ \text{ for } j > 2n. \tag{12b}$$

And then the magnitudes of the eigenvalues for TVFAR are

$$|\bar{\lambda}_i| \leqslant 1{\cdot}0 \ \text{ for } i \leqslant 2n \quad \text{and} \quad |\bar{\lambda}_j| > 1{\cdot}0 \ \text{ for } j > 2n. \tag{12c}$$

For TVFAR model the first $2n$ eigenvalues located inside or on the unit circle are attributed to the system modes, and the leftover $pq - 2n$ eigenvalues located outside the unit circle are the spurious modes. It should be mentioned here that all of the eigenvalues from common forward AR model locate inside the unit circle.

The state equation derived from the proposed VBAR model provides a determinate boundary to distinguish the system modes from spurious modes.

The reduced order state-space model in discrete time with size of $2n$, which is represented by (A_d, B_d, C_d, D_d), can be constructed by removing the corresponding columns and rows of $pq - 2n$ spurious modes in the transformed forward state equation (see Appendix A). Then the state-space system can be transformed into a continuous time model, represented by (A_c, B_c, C_c, D_c), as follows [28]:

$$A_c = ln(A_d)/\Delta t, \qquad B_c = A_c(A - I)^{-1}B_d, \tag{13a,b}$$

$$C_c = C_d, \qquad D_c = D_d. \tag{13c,d}$$

3. EXTRACTION OF MODEL PARAMETERS

The equation of motion for a structure system with n degrees of freedom under the exciting force can be expressed by

$$M\ddot{y}(t) + E\dot{y}(t) + Ky(t) = B_0u(t) \tag{14}$$

where t is the continuous time, $y(t)$ is the $n \times 1$ displacement vector, $u(t)$ is the $nH1$ force vector, M is the $n \times n$ positive-definite mass matrix, E is the $n \times n$ positive-semidefinite damping matrix, K is the $n \times n$ positive-semidefinite stiffness matrix, and B_0 is the $n \times n$ input matrix. The dots denote differentiation with respect to time. In the practical experimental identification of dynamic characteristics of structures, not all of the degrees of freedom are observed. For a measurement system with p sensors on structures, if the sensors for displacement, velocity, and acceleration are arranged on different locations to measure the different types of dynamic responses simultaneously, then the output equation of the structural system for combined displacement, velocity and acceleration (DVA) measurements can be expressed as [28, 29]

$$y(t) = \tilde{C}_d x(t) + \tilde{C}_v\dot{x}(t) + \tilde{C}_a\ddot{x}(t), \tag{15}$$

where $\tilde{C}_d, \tilde{C}_v, \tilde{C}_a \in R^{p \times n}$ are the output influence matrices of displacement, velocity and acceleration respectively. After introducing the state vector, $z(t) = \{x(t), \dot{x}(t)\} \in R^{2n \times 1}$, the equations of motion for the physical model described by equation (14) can be transformed into the following state equation of motion:

$$\dot{z}(t) = Az(t) + Bu(t), \tag{16}$$

where $A \in R^{2n \times 2n}$ is the system matrix, $B \in R^{2n \times n}$ is the input matrix, and

$$A = \begin{bmatrix} 0 & I \\ -M^{-1}K & -M^{-1}E \end{bmatrix}, \qquad B = \begin{bmatrix} 0 \\ M^{-1}B_0 \end{bmatrix} \tag{17a,b}$$

The output equation in equation (15) can be transformed as

$$y(t) = Cz(t) + Du(t), \tag{18}$$

where

$$C = [\tilde{C}_d - \tilde{C}_a M^{-1} K \quad \tilde{C}_v - \tilde{C}_a M^{-1} E], \quad D = \tilde{C}_a M^{-1} B_0. \tag{19a,b}$$

Here, $C \in R^{p \times 2n}$ is the output influence matrix of the state vector $z(t)$, $D \in R^{p \times n}$ is the direct transmission matrix. The matrix D will disappear from equation (18) when acceleration is not used as measured output.

When the input information is absent, from the measured response data we can identify the equivalent state system matrix A_c and the output influence matrix C_c only. The matrices B_c and D_c have no effect on the extraction of modal parameters. The natural frequencies and mode shapes can be computed from the eigenanalysis of the system matrix A in equation (17a). The eigenanalysis of the identified equivalent system matrix A_c in equation (13a) should provide the same results for a noise-free system. The natural frequencies and damping ratios in terms of the eigenvalues ($s_i = \alpha_i + j\beta_i$, $i = 1, 2, \ldots, n$) of A or A_c are

$$\omega_i = \sqrt{\alpha_i^2 + \beta_i^2}, \qquad \xi_i = \alpha_i / \omega_i \tag{20a,b}$$

The normal mode shapes are the eigenvectors of the matrix $M^{-1}K$, which appears in the left-lower block of matrix A. Although the identified system matrix A_c has the same modal parameters as matrix A, however, the distribution of the elements in these two matrices are different, i.e., the left-upper block in matrix A_c is not a zero matrix and the right-upper block is not a diagonal unit matrix. Therefore, the normal modes cannot be calculated from the left-lower block of identified A_c directly. Hung *et al.* [29] proposed a transformation matrix T that can transform the identified system matrix A_c into a matrix with the same type as matrix A. The transformation matrix can be expressed in terms of the identified A_c and C_c together with the output influence matrices for displacement, velocity and acceleration as follows:

$$T = \begin{bmatrix} T_1 \\ T_2 \end{bmatrix}, \tag{21}$$

where

$$T_1 = \tilde{C}_d C_c + \tilde{C}_v C_c A_c^{-1} + \tilde{C}_a C_c A_c^{-2}, \qquad T_2 = T_1 A_c. \tag{22a,b}$$

The identified system matrix $\bar{A}$ that has the same type as physical system matrix A in equation (17a) can be obtained by the following transformation:

$$\bar{A} = T A_c T^{-1}. \tag{23}$$

When only one of the displacement, velocity and acceleration is available to be measured, the transformation matrices are

$$T = T_d = \begin{bmatrix} C_c \\ C_c A_c \end{bmatrix} \quad \text{for displacement only,} \tag{24a}$$

$$T = T_v = T_d A_c^{-1} = \begin{bmatrix} C_c A_c^{-1} \\ C_c \end{bmatrix} \quad \text{for velocity only,} \tag{24b}$$

$$T = T_a = T_d A_c^{-2} = \begin{bmatrix} C_c A_c^{-2} \\ C_c A_c^{-1} \end{bmatrix} \quad \text{for acceleration only.} \tag{24c}$$

The normal model shapes are the eigenvectors of the negative submatrix of left-lower block of matrix $\bar{A}$.

4. NUMERICAL EXAMPLE

In order to illustrate the availability of the proposed VBAR approach, a lumped mass model with three d.o.f. shown in Figure 1 is selected as a study case. The parameters of this model are: $m_1 = 1$, $m_2 = 2$, $m_3 = 3$, $c_1 = c_4 = c_5 = 0{\cdot}1$, $c_2 = c_3 = 0{\cdot}2$, $k_1 = 10$, $k_2 = 20$ and $k_3 = 30$. The system is excited by a random non-zero initial condition. For reference purpose, the fourth order Runge–Kutta method was employed to calculate the displacement, velocity and acceleration at m_1, m_2 and m_3, respectively, and the calculated dynamic responses are used as the true values. The sampling rate of the time series data was 5 Hz, and the short data record of 256 data points of displacement, velocity and acceleration were picked. The time histories of response for different sensors at different positions are shown in Figure 2. The time histories of magnitude and change rate of the measured displacement, velocity and acceleration are obviously different. To examine the effects of noise on the accuracy of the identified modal parameters, a zero mean white noise with 20% r.m.s. of measured response was added to the noise-free response data to simulate the measurement noise.

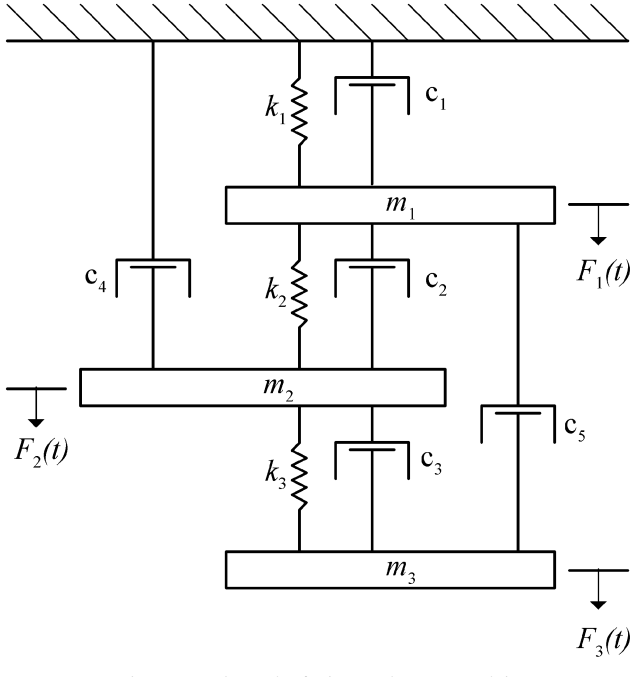

Figure 1. Three d.o.f.s lumped mass model.

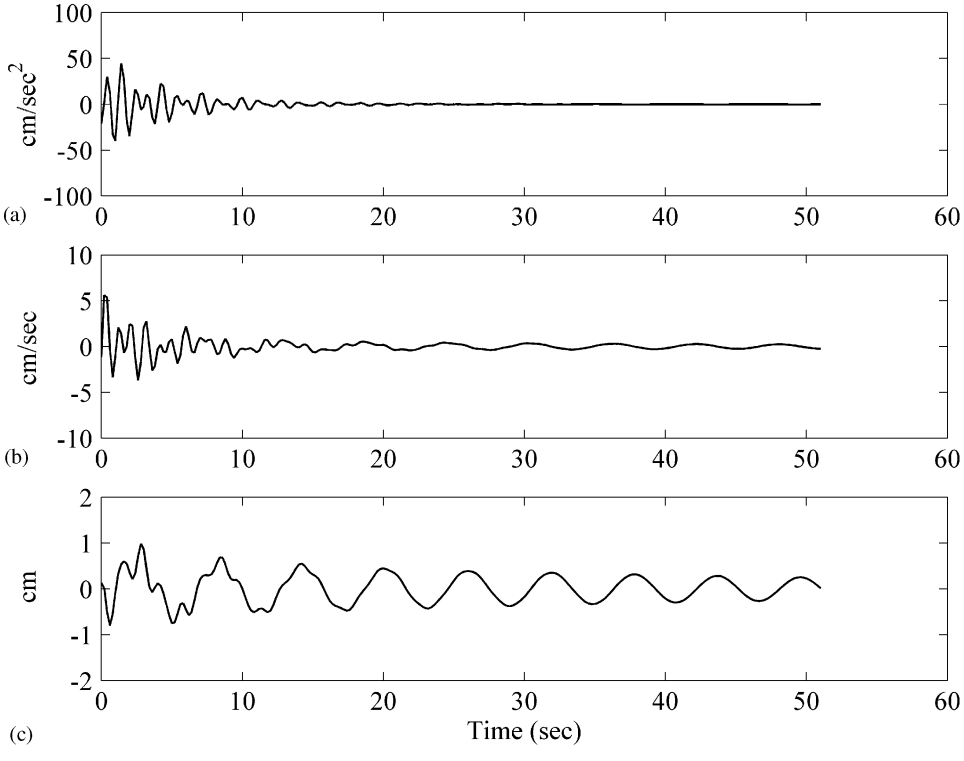

Figure 2. Time history responses of three d.o.f.s model. (a) acceleration at m_1; (b) velocity at m_2; (c) displacement at m_3.

In order to show the advantage of the proposed method on the selection of system order and model reduction, the stochastic subspace identification (SSI) algorithm is used as a comparative case. For the concept and procedure of modal identification using the SSI algorithm, please refer to the literature of Overschee and Moor [14, 15]. The SSI algorithm determines the model order by the singular value decomposition (SVD) technique of a weighted projection matrix, and reduces the model by selecting the dominant singular values (DSV). Figure 3 shows the distribution of singular value calculated by the SSI algorithm with 15 block rows in the case of 20% noise level. The total number of singular values is 45. The SVD based algorithm may fail to find out the exact mode order. Figure 3 shows that there are at least three gaps in the singular plots. The number of dominant singular values may be two, four or six depending upon the subjective selection of the user. On the contrary, the proposed VBAR approach uses the border of unit circle to select the structure eigenvalues from all computed eigenvalues.

In order to compare with the SSI algorithm the order of the AR model was selected as 15. The distribution of computed 45 eigenvalues by common VFAR method and the TVFAR approach is shown in Figure 4. It shows that both models provide the same system eigenvalues; however, all of the eigenvalues computed by the common VFAR method locate inside the unit circle; and it is not easy to discriminate the system modes from spurious modes directly. On the other hand, the eigenvalues computed by the proposed approach are divided into two parts, the points located inside the unit circle are the identified system modes, and the others located outside the unit circle are the spurious modes. It is clear that the number of system modes determined by the eigenvalue filter is six.

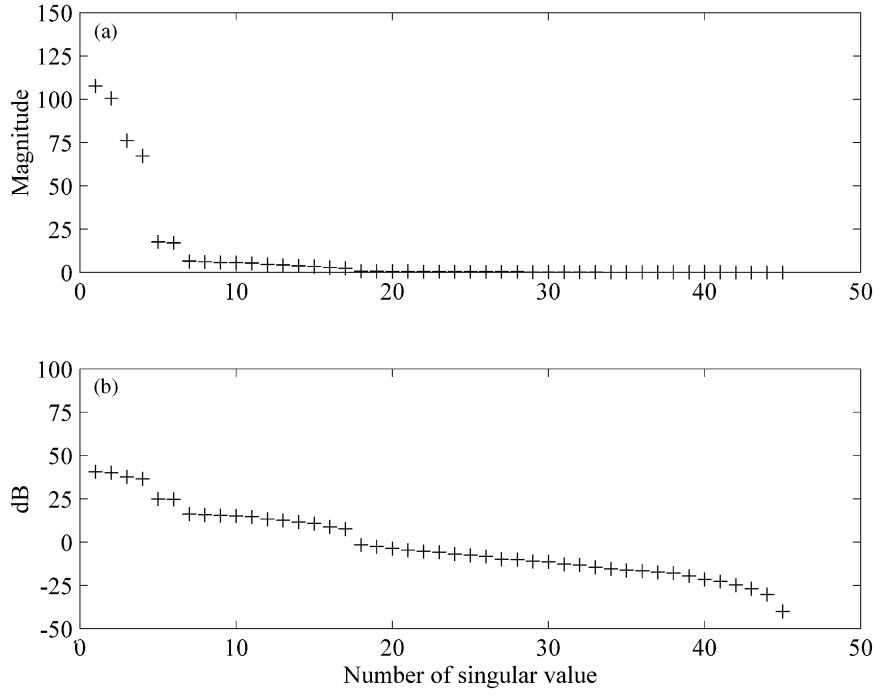

Figure 3. Distribution of singular value for 15 block rows (20% noise level). (a) Magnitude (b) logarithm.

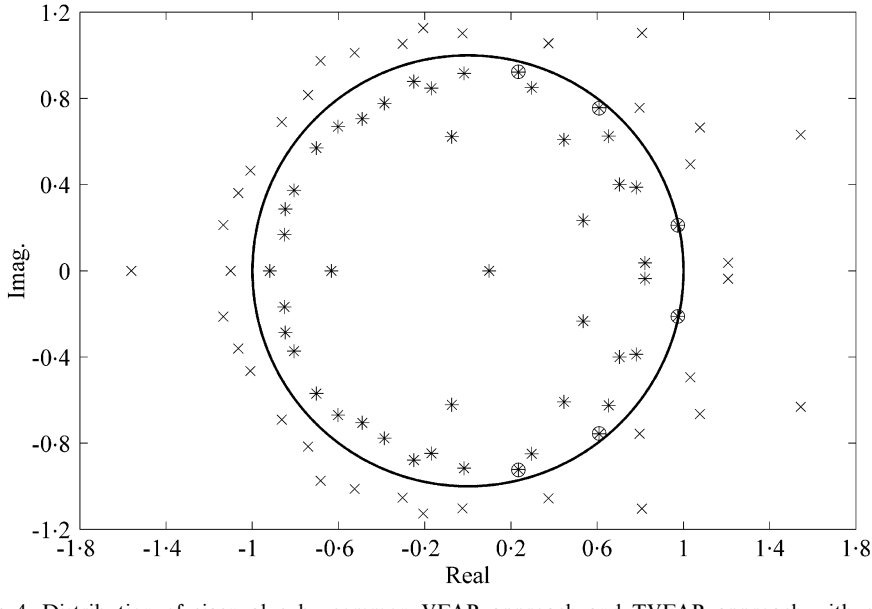

Figure 4. Distribution of eigenvalue by common VFAR approach and TVFAR approach with order 15 (20% noise level). *, VFAR; ○ and ×, TVFAR.

Table 1 shows the comparison of the identified natural frequencies and damping ratios between the proposed approach and the SSI algorithm with various selections of dominant singular values (DSV). When the number of selected DSV is not adequate in the SSI approach, the identified modal parameters may have notable errors.

TABLE 1

Comparison of identified natural frequencies (Hz) and damping ratios (%) by VBAR (3,15) and SSI methods (20% noise level)

Mode	True		VBAR(3,15)		SSI(15)					
					DSV = 2		DSV = 4		DSV = 6	
	ω_i	ξ_i	ω_i	ξ_i	ω_i	ξ_i	ω_i	ξ_i	ω_i	ξ_i
1	0·1699	1·7626	0·1702	1·6530	N.A.	N.A.	N.A.	N.A.	0·1700	0·5127
2	0·7120	3·4783	0·7109	3·4812	N.A.	N.A.	0·7116	3·5052	0·7124	3·4800
3	1·0537	3·7849	1·0535	3·6449	0·9341	6·6453	1·0524	3·8664	1·0524	3·8492

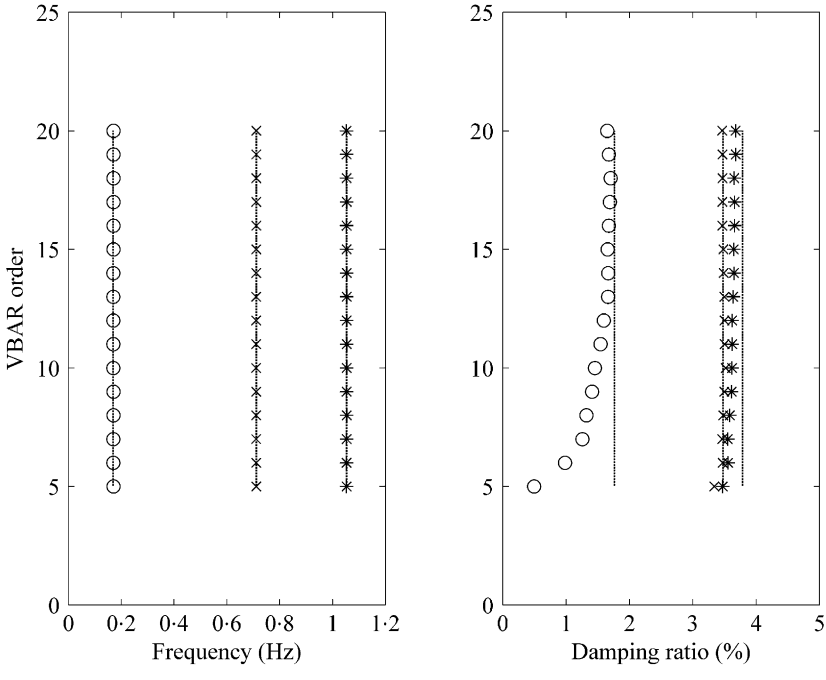

Figure 5. Identified natural frequencies and damping ratios versus VBAR order.

Figure 5 shows the distribution of the identified natural frequencies and damping ratio versus model order by the proposed method. Straight dotted lines indicate the true values. Although the selection of the number of dominant singular values is not easy in the SSI approach under high noise background, a preselected DSV number is set to six for comparing with the proposed VBAR method. Figure 6 shows the results by subspace approach. The results show that increase of the order for VBAR model and the number of block rows for SSI method can improve the accuracy of the identified modal parameters. Both methods have superior ability in identifying the natural frequencies, but the identified damping ratio of the first mode using SSI method seems to fail in convergence. Modal assurance criterion (MAC) can roughly evaluate the accuracy of the identified mode shape. Figure 7 shows the MAC of the identified first mode shape, it shows that the identified mode shape by the proposed method is better than by SSI method in high level of noise.

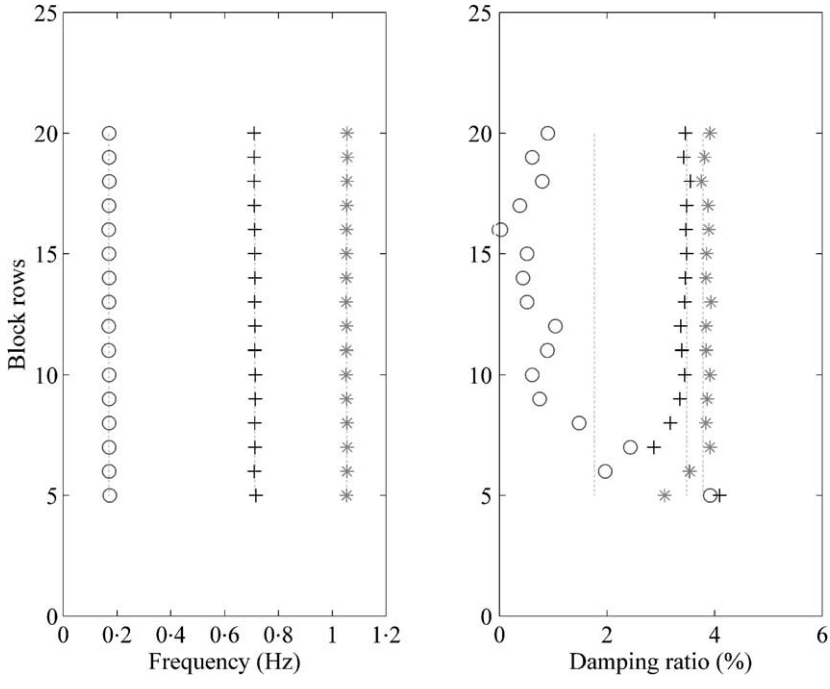

Figure 6. Identified natural frequencies and damping ratios versus number of block rows using SSI approach.

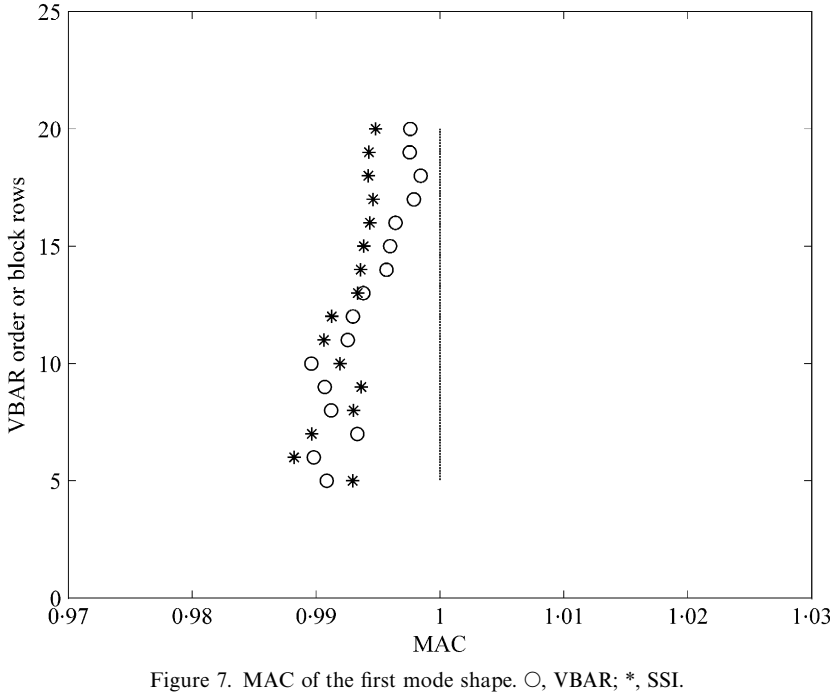

Figure 7. MAC of the first mode shape. ○, VBAR; *, SSI.

5. EXPERIMENTAL EXAMPLE AND DISCUSSION

The experimental modal identification of a vertical cantilever beam shown in Figure 8 was set up with four measurement points. The cantilever has a rectangular cross-section; the geometric and material properties are listed in Table 2. Three Keyence LB-70/LB-11 and one LB-081/LB-1101 laser displacement meters were employed to measure the displacement response as shown in Figure 8. The PCB modally tuned impulse hammer was used to hit the top of the beam transversely (point 4 in Figure 8). The response signals were fed through a set of controllers to a multi-channel A/D converter at a sampling rate of 360 Hz, and 1024 data points were taken for each channel.

The distribution of logarithm of singular value calculated by stochastic subspace identification (SSI) method in 20, 30, 40 and 50 block rows are shown in Figure 9. It is difficult to guess the actual number of DSV from different block rows. Figure 10 shows the distribution of eigenvalues identified by the proposed TVFAR with order 20. The first 20 eigenvalues and their magnitude in the ascending order are listed in Table 3. From Figure 10 and Table 3, it is very obvious that the proposed approach can easily recognize the number of system eigenvalues to be eight. Figure 11 and Table 4 show the distribution of eigenvalues and their first 20 eigenvalues identified by TVFAR with order 40. There are a total of 160 eigenvalues, but only 8 of them are the system modes.

In this example the sampling rate of measured data series is 360 Hz, and the analysis bandwidth of frequency is 180 Hz. Although the number of vibration modes of the continuous beam is theoretically infinite, the number of vibration modes below 180 Hz is only four, therefore only four pairs of conjugate complex roots can be found. When the sampling rate of measured data is increased, more pairs of system modes will be identified if the order of VBAR model is adequate. The characteristic roots of equations (3) and (10) associated with higher damping ratios are farther from the unit circle, and therefore the proposed approach is effective in a dynamical system with large damping ratios.

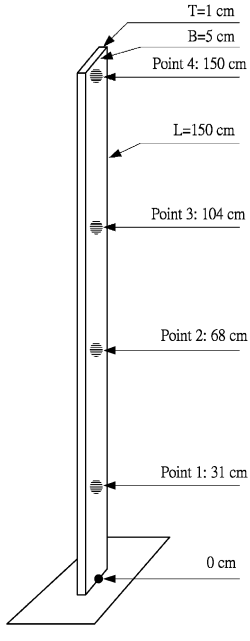

Figure 8. Experimental arrangement of cantilever steel beam.

TABLE 2

Geometric and material properties of cantilever beam

Parameters	Value
Length L, (cm)	150
Width B (cm)	5
Thickness T (cm)	1
Young's modulus E (Gpa)	190
Mass density ρ (Kg/m^3)	7850

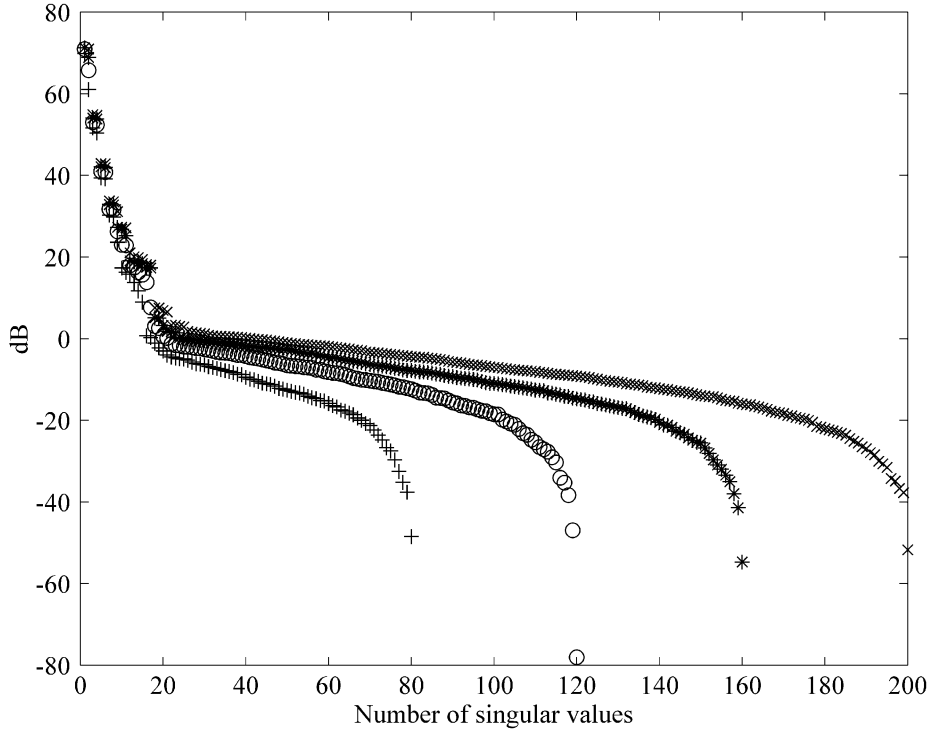

Figure 9. Distribution of singular values for various block rows (cantilever beam). +, 20; ○, 30; *, 40; ×, 50.

Figures 12–15 show the relationship between the identified natural frequency, and the order for VBAR method or block rows for SSI methods. In each selected block row, the DSV is set to 8 compared with 8 system modes of VBAR model. The results show that the modes identified by VBAR method are more stable than by SSI method. If the model order is high enough, the eigenvalue filter for VBAR method can separate all system modes from spurious modes. The higher order of model can increase the accuracy of te identified modal parameters.

Table 5 lists four identified natural frequencies and damping ratios by VBAR with order 40 and the natural frequencies by Euler–Bernoulli beam theory without damping. Figure 16 shows four identified relative mode shapes and the mode shapes obtained by beam theory. The distribution of power spectrum density of the measured data at position 1 shown in Figure 17 can verify these modes that have been identified.

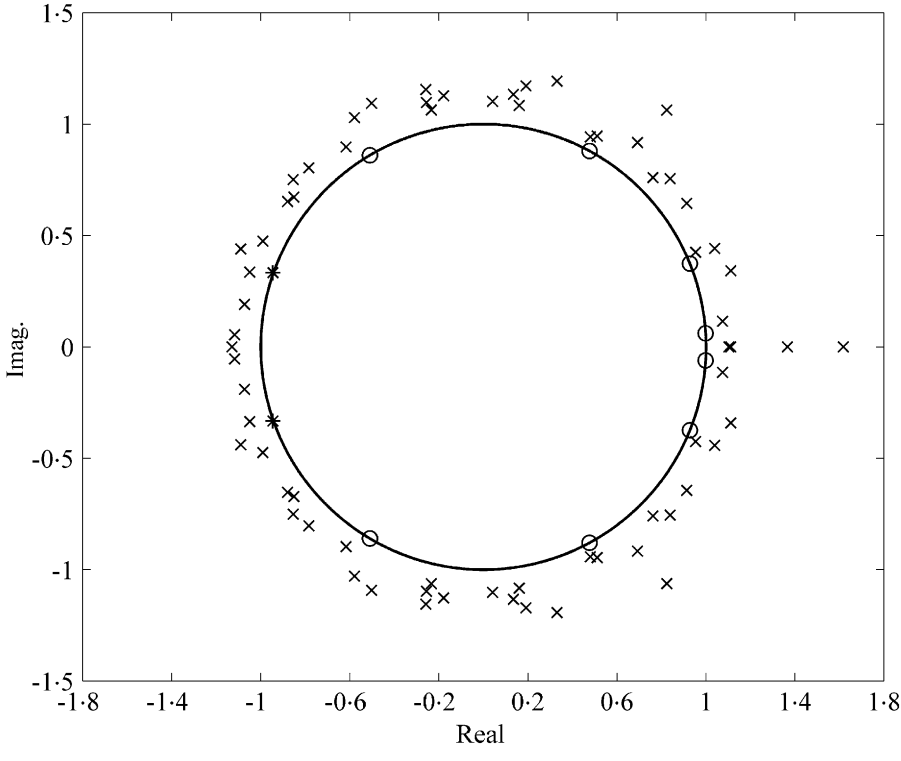

Figure 10. Distribution of eigenvalue by TVFAR(4, 20) (cantilever steel beam).

TABLE 3

The first 20 *eigenvalues and their magnitudes of cantilever beam by TVFAR* (4,20)

Eigenvalue modes 1–10	Magnitude modes 1–10	Eigenvalue modes 11–20	Magnitude modes 11–20
0·4761 − 0·8787i	0·999397	0·9529 − 0·4249i	1·043367
0·4761 + 0·8787i	0·999397	0·9529 + 0·4249i	1·043367
−0·5099 − 0·8598i	0·999598	0·4801 − 0·9422i	1·057445
−0·5099 + 0·8598i	0·999598	0·4801 + 0·9422i	1·057445
0·9273 − 0·3740i	0·999867	0·5105 − 0·9457i	1·074696
0·9273 + 0·3740i	0·999867	0·5105 + 0·9457i	1·074696
0·9981 − 0·0607i	0·999953	0·7611 − 0·7592i	1·075007
0·9981 + 0·0607i	0·999953	0·7611 + 0·7592i	1·075007
−0·9454 − 0·3329i	1·002326	1·0740 − 0·1146i	1·080109
−0·9454 + 0·3329i	1·002326	1.0740 + 0·1146i	1·080109

6. CONCLUSION

In this paper, a vector backward AR model to identify the modal parameters from output data of multi-channel measurement system has been examined. The proposed method not only identifies the natural frequency and damping ratio accurately, but also extracts the relative mode shapes. The key advantage of the proposed VBAR approach is that the

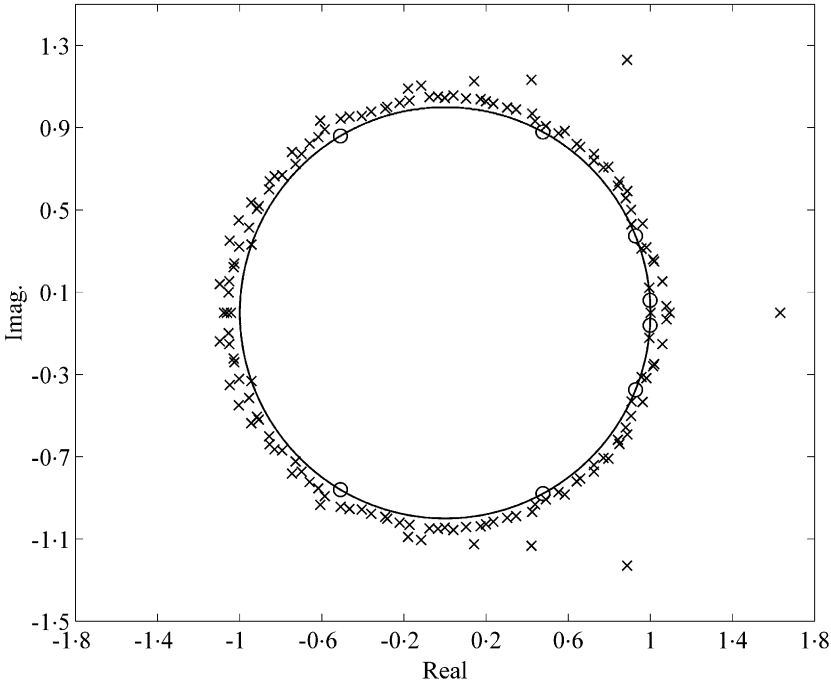

Figure 11. Distribution of eigenvalue by TVFAR(4,40) (cantilever steel beam).

TABLE 4

The first 20 *eigenvalues and their magnitudes of cantilever beam by TVFAR* (4,40)

Eigenvalue modes 1–10	Magnitude modes 1–10	Eigenvalue modes 11–20	Magnitude modes 11–20
0·4761 − 0·8787i	0·999389	1·0008	1·000768
0·4761 + 0.8787i	0·999389	0·9940 − 0·1218i	1.001468
−0·5098 − 0·8598i	0·999573	0·9940 + 0.1218i	1·001468
−0·5098 + 0·8598i	0·999573	0·9076 − 0·4311i	1·004748
0.9273 − 0·3740i	0·999861	0·9076 + 0·4311i	1·004748
0·9273 + 0·3740i	0.999861	0·9563 − 0·3123i	1·006044
0.9981 − 0·0607i	0·999957	0·9563 + 0·3123i	1·006044
0·9981 + 0·0607i	0·999957	−0·7286 − 0·7227i	1·026257
−0·9436 − 0·3317i	1·000141	−0·7286 + 0·7227i	1·026257
−0·9436 + 0·3317i	1·000141	0·4382 − 0·9317i	1·029576

system eigenvalues can be separated clearly from the spurious modes using the boundary of unit circle.

The proposed VBAR model can be transformed to TVFAR model to extract the system matrices for the equation of motion of physical model. And it has the same possible applications as the common forward AR approach.

In the numerical example, a noise level in 20% r.m.s. of measurement data are taken into consideration. The results of numerical and experimental examples show that determination of the number of system modes using SVD-based method is not easy without using the prior information of structure or other useful criteria. The proposed VBAR model

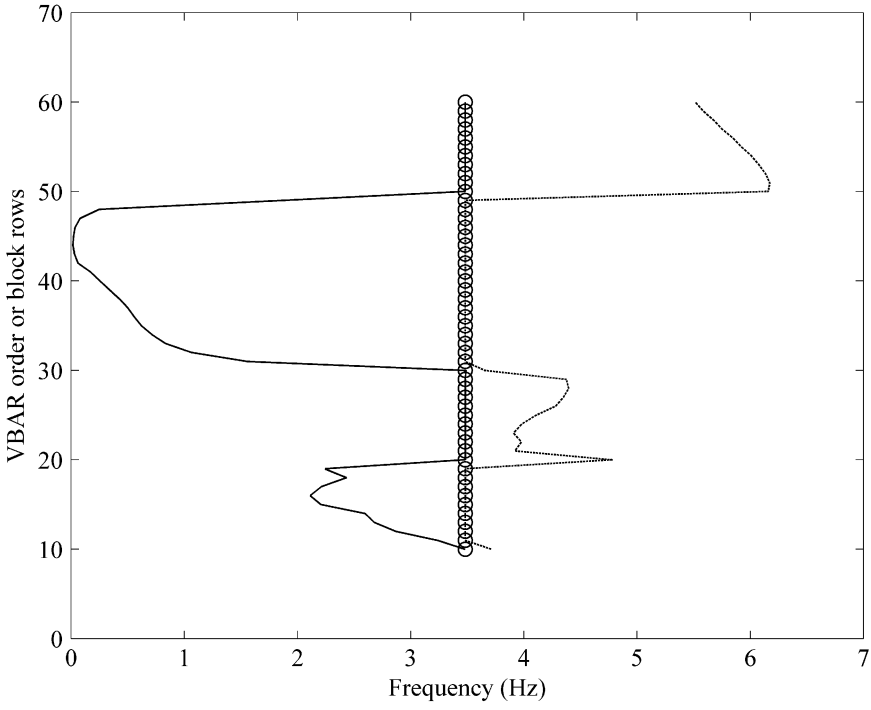

Figure 12. Natural frequencies versus the order of VBAR or block rows of SSI (cantilever steel beam). ○, first mode by VBAR; —— and – – – for first and second modes by SSI.

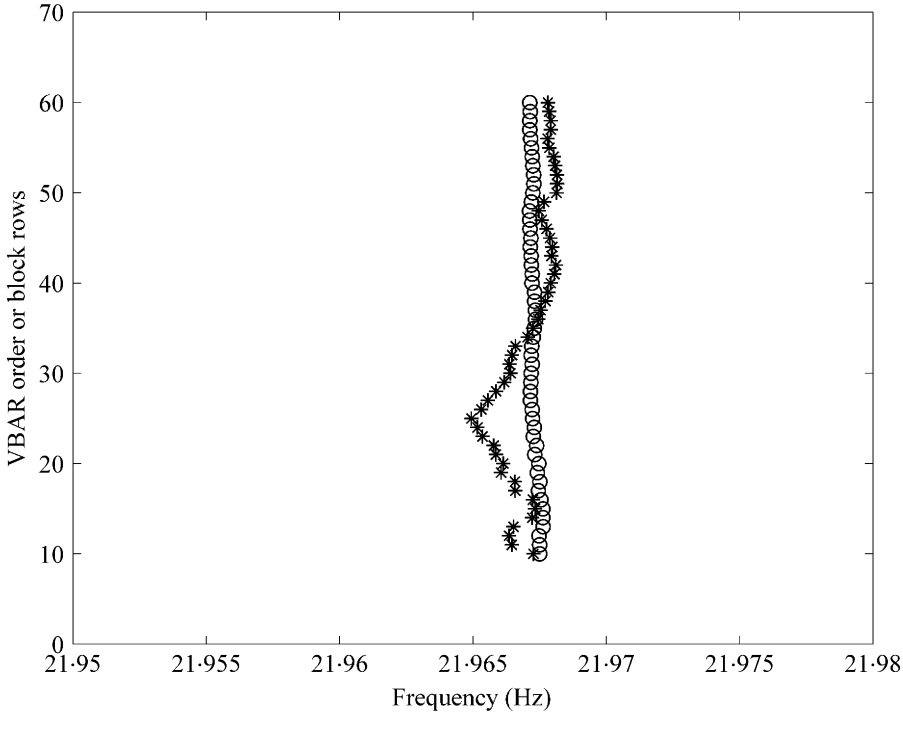

Figure 13. Natural frequencies versus the order of VBAR or block rows of SSI (cantilever steel beam). ○, second mode by VBAR; *, third mode by SSI.

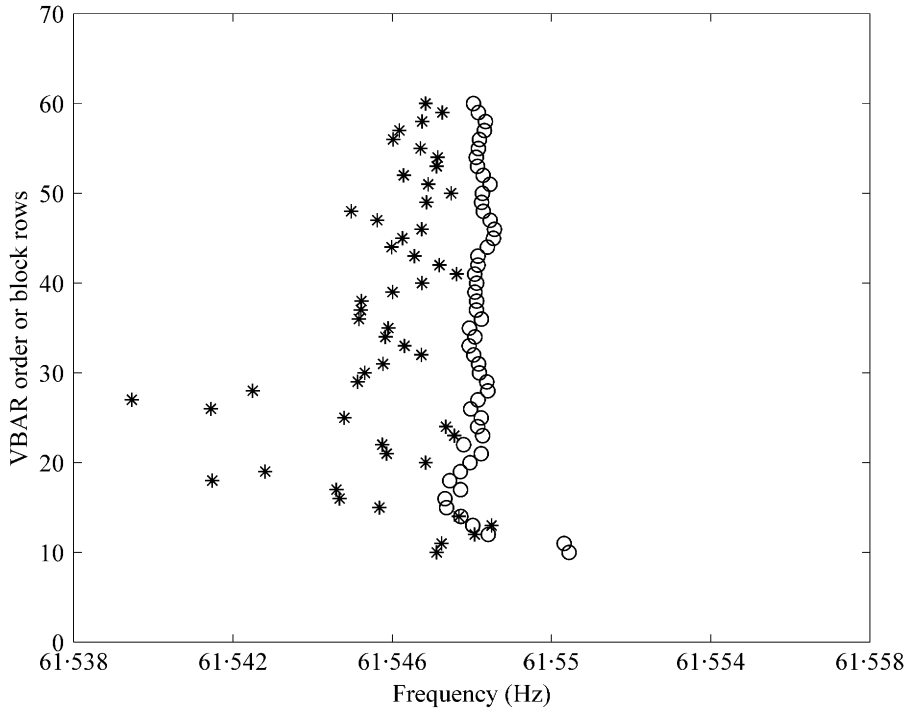

Figure 14. Natural frequencies versus the order of VBAR or block rows of SSI (cantilever steel beam). ○, third mode by VBAR; *, fourth mode by SSI.

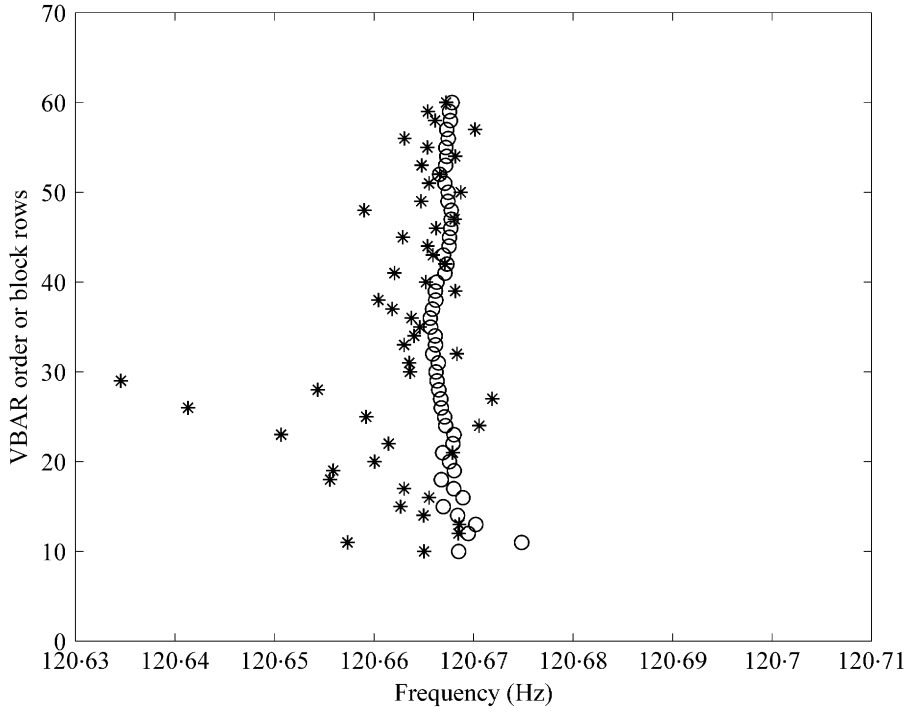

Figure 15. Natural frequencies versus the order of VBAR or block rows of SSI (cantilever steel beam). ○, fourth mode by VBAR; *, fifth mode by SSI.

TABLE 5

Comparison of natural frequencies (Hz) and damping ratios (%) by Euler–Bernoulli beam theory and by VBAR(4,40) model

Mode	E − L theory	Identified by VBAR(40)	
	ω_i	ω_i	ξ_i
1	3·5322	3·4826	0·0707
2	22·1356	21·9672	0·0364
3	61·9804	61·5481	0·0569
4	121·4569	120·6663	0·0203

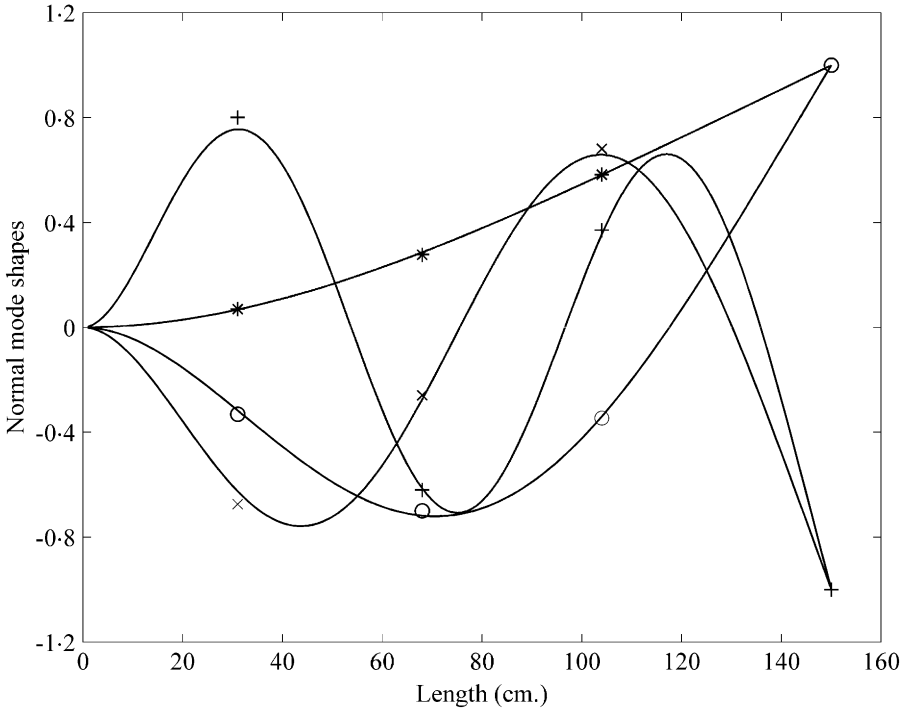

Figure 16. The relative mode shapes. —— for analytical solution; *, first mode; ○, second mode; × ○, third mode; + ○, fourth mode.

can easily determine the order of system modes directly. Although the numerical and experimental examples in this paper only used the free response data for the identification of modal parameters, the application can be extended to the cases for ambient vibration, or forced response excited by unknown white noise.

ACKNOWLEDGMENTS

The authors gratefully acknowledge the financial support of the National Science Council, Republic of China, under project numbers NSC 88-2611-E-002-008 and NSC 89-2611-E-002-007.

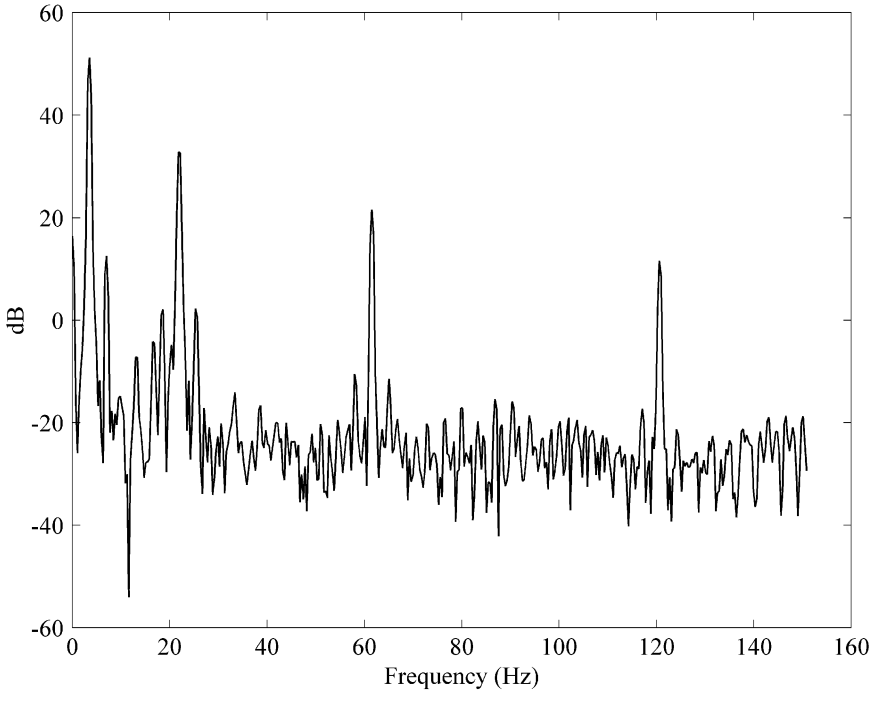

Figure 17. The power spectrum density of measured displacement at point 1 of cantilever steel beam.

REFERENCES

1. R. Provasi and G. A. Zanetta 2000 *Mechanical System and Signal Processing* **14**, 327–341. The extended Kalman filter in the frequency domain for the identification of mechanical structures excited by sinusoidal multiple inputs.
2. M. B. Tischler 1985 *NASA Technical Memorandum* 110369, *USAATCOM Technical Report* 95-A-007. System identification methods for aircraft control development and validation.
3. S. R. Ibrahim and E. C. Mikulcik 1973 *Shock and Vibration Bulletin* **43**. A time domain vibration test.
4. S. R. Ibrahim 1978 *Journal of Spacecraft and Rockets* **15**, 313–316. Modal confidence factor in vibrating testing.
5. F. Deblauwe, D. L. Brown and R. J. Allemang 1987 *5th International Modal Analysis Conference Society for Experimental Mechanics, London, UK*, 832–842. The polyreference time domain technique.
6. J. M. Leuridan, D. L. Brown and R. J. Allemang 1986 *Journal of Vibration, Acoustics, Stress, and Reliability in Design* **108**, 1–8. Time domain parameter identification methods for linear modal analysis.
7. F. Lembregt and R. Snoeys 1987 *International Journal of Analytical and Experimental Modal Analysis* **2**, 19–31. Application and evaluation of multiple-input modal parameter estimation.
8. J. N. Juang and R. S. Pappa 1985 *Journal of Guidance, Control, and Dynamics* **8**, 620–627. An eigensystem realization algorithm for modal parameter identification and model reduction.
9. J. N. Juang and R. S. Pappa 1986 *Journal of Guidance, Control, and Dynamics* **9**, 294–303. Effect of noise on modal parameters identified by the eigensystem realization algorithm.
10. D. A. Pierre, D. J. Trudnowski and J. F. Hauer 1992 *IEEE Transaction on Automatic Control* **37**, 831–835. Identifying linear reduced models for system with arbitrary initial conditions using Prony signal analysis.
11. C. S. Li and W. J. Ko 1988 *The Royal Institution of Naval Architects* **130**, 315–327. On the application of the time series in structural failure detection and monitoring for offshore applications.

12. N. P. MEHTA and S. M. PANDIT 1991 *Journal of Vibration and Acoustics* **113**, 416–417. Modal analysis of multiple eigenvalue system by dynamic data systems.
13. C. S. LI, W. J. KO, H. T. LIN and R. J. SHYU 1993 *Journal of Sound and Vibration* **167**, 1–15. Vector autoRegressive model analysis with application to ship structures.
14. P. VAN OVERSCHEE and B. DE MOOR 1992 *Recent Advances in Mathematical Theory of System, Control, Networks and Signal Processing* **1**, 589–594. Subspace algorithms for system identification and stochastic realization.
15. P. VAN OVERSCHEE and B. DE MOOR 1996 *Subspace Identification for Linear Systems, Theory—implementation—applications*. Dordrecht: Kluwer Academic Publishers.
16. C. F. CREMONA and J. A. BRANDON 1992 *Mechanical System and Signal Processing* **6**, 229–236. Model order testing in discrete time domain identification methods.
17. L. D. PETERSON and K. F. ALVIN 1997 *Journal of Sound and Vibration* **201**, 137–144. Time and frequency domain procedure for identification of structural dynamic models.
18. T. SODERSTROM 1989 *System Identification*. U.K., Cambridge: Prentice-Hall.
19. S. M. KAY 1988 *Modern Spectral Estimation—Theory and Application*. Englewood Cliffs, NJ: Prentice-Hall.
20. X. HE and G. DE ROECK 1997 *Computers and Structures* **64**, 341–353. System identification of mechanical structures by a high-order multivariate autoregressive model.
21. C. F. HUNG, W. J. KO and C. H. TAI 1998 *Journal of Society of Naval Architecture and Marine Engineering, ROC* **17**, 35–44. Identification of modal parameters by the state equation of vector auto-regressive model (in Chinese).
22. R. KUMARESAN and D. W. TUFTS 1982 *IEEE Transactions on Acoustics, Speech, and Signal Processing* **30**, 833–840. Estimating the parameters of exponentially damped sinusoids and pole-zero modeling in noise.
23. J. J. HOLLKAMP and S. M. BATILL 1991 *American Institute of Aeronautics and Astronautics Journal* **29**, 96–103. Automated parameter identification and order reduction for discrete time series models.
24. J. E. COOPER 1992 *Mechanical System and Signal Processing* **6**, 217–228. The use of backwards model for structural parameters identification.
25. M. M. A. WAHAB and G de ROECK 1999 *Mechanical System and Signal Processing* **13**, 449–474. An effective method for selecting physical modes by vector autoregressive models.
26. C. S. HUANG 2001 *Journal of Sound and Vibration* **241**, 337–359. Structural identification from ambient vibration measurement using the multivariate AR model.
27. I. GOHBERG, P. LANCASTER and L. RODMAN 1982 *Matrix Polynomials*. New York: Academic Press.
28. J. N. JUANG 1994 *Applied System Identification*. Englewood Cliffs, NJ: Prentice-Hall, PTR.
29. C. F. HUNG, W. J. KO and C. H. TAI 2000 *The First International Conference on Structural Stability and Dynamics. Taipei, Taiwan, December* 7–9. Identification of modal parameters from the combined DVA measured data under unknown input force.

APPENDIX

A discrete time state-space system with size pq can be expressed as

$$\hat{z}_{t+1} = a\hat{z}_t + b\hat{\varepsilon}_t, \qquad y_t = c\hat{z}_t + d\hat{\varepsilon}_t. \tag{A.1, 2}$$

The state system matrix a can be decomposed as follows:

$$a = P\Lambda P^{-1} = \begin{bmatrix} P_{ss} & P_{sp} \\ P_{ps} & P_{pp} \end{bmatrix} \begin{bmatrix} \Lambda_s & 0 \\ 0 & \Lambda_p \end{bmatrix} \begin{bmatrix} P_{ss} & P_{sp} \\ P_{ps} & P_{pp} \end{bmatrix}^{-1}, \tag{A.3}$$

where the subscripts s and p indicate the system and spurious mode respectively. Λ_s and Λ_p are the diagonal sub-matrices that contain the $2n$ system eigenvalues and $pq - 2n$ spurious eigenvalues respectively.

Let $\hat{x}_t = P^{-1}\hat{z}_t$, and then $\hat{z}_t = P\hat{x}_t$.

Multiplied by P^{-1} equation (A.1) becomes

$$\hat{x}_{t+1} = P^{-1}\hat{z}_{t+1} = P^{-1}P\Lambda\ P^{-1}\hat{z}_t + P^{-1}b\varepsilon_t = \Lambda\hat{x}_t + P^{-1}b\varepsilon_t. \tag{A.4}$$

The state vector can be divided into system and non-system parts, and equations (A.1) and (A.2) can be rewritten as follows:

$$\hat{x}_{t+1} = \begin{Bmatrix} \hat{x}^s_{t+1} \\ \hat{x}^p_{t+1} \end{Bmatrix} = \begin{bmatrix} \Lambda_s & 0 \\ 0 & \Lambda_p \end{bmatrix} \begin{Bmatrix} \hat{x}^s_t \\ \hat{x}^p_t \end{Bmatrix} + \begin{bmatrix} b_s \\ b_p \end{bmatrix} \hat{\varepsilon}_t, \quad y_t = [c_s \quad c_p] \begin{Bmatrix} \hat{x}^s_t \\ \hat{x}^p_t \end{Bmatrix}_t + d\hat{\varepsilon}_t, \tag{A.5, 6}$$

where

$$\begin{bmatrix} b_s \\ b_p \end{bmatrix} = P^{-1}b, \qquad [c_s\ c_p] = cP. \tag{A.7, 8}$$

Neglecting the affection of spurious modes in $\hat{z}_t = P\hat{x}_t$, the state vector of system part can be approximated as $\hat{z}^s_t \approx p_{ss}\hat{x}^s_t$, and then $\hat{x}^s_t \approx p^{-1}_{ss}\hat{z}^s_t$.

The state equation and output equation of the reduced order system with size $2n$ can be expressed as follows

$$\hat{z}^s_{t+1} = A_d\hat{z}^s_t + B_d\varepsilon^s_t, \quad y_t = C_d\hat{z}^s_t + D_d\varepsilon^s_t, \tag{A.9, 10}$$

where $A_d = P_{ss}\Lambda_s P^{-1}_{ss}$, $B_d = P_{ss}b_s$, $C_d = c_s P^{-1}_{ss}$, $D_d = d$ (A.11–14)